Jordan Journal of Civil Engineering, Volume **18**, No. **4**, **2024**
DOI: https://doi.org/10.14525/JJCE.v18i4.12

Jordan Journal of Civil Engineering

Journal homepage: https://jjce.just.edu.jo

Parametric Study of Mechanically Stabilized Earth Wall Using Finite Element Analysis

Moamen Abd El Raouf [1)*] ***and Khaled M.M. Bahloul*** [2)]

[1)] *Civil Engineering Department, Faculty of Engineering, Al-Azhar University, Qena, Egypt.*
** Corresponding Author. E-Mail: moamenabdelmontaleb@azhar.edu.eg*
[2)] *Lecturer, Department of Construction Engineering, October High Institute of Engineering and Technology, Egypt.*

ARTICLE INFO

Article History:
Received: 22/2/2024
Accepted: 5/10/2024

ABSTRACT

Mechanically Stabilized Earth (MSE) walls must be carefully designed and constructed to obtain satisfactory stability. The reinforced soil structures are more flexible and ductile. Therefore, it is more capable of resisting seismic load and differential settlement. In this paper, the influence of some parameters on the horizontal displacement and axial force of the Mechanically Stabilized Earth (MSE) walls is investigated. The studied parameters include the constitutive models, the axial geogrid stiffness, and the secondary reinforcement length. From the numerical analysis, it was found that the hardening soil model with small strain (HSS) predictions is more realistic than the results obtained from the traditional Mohr-Columb (MC) model and the hardening soil (HS) model. Moreover, a reduction in the relative deflection of the wall facing was observed with an increase in the axial geogrid stiffness. Also, the maximum axial force in the reinforcement increased with an increase in the axial geogrid stiffness. Moreover, increasing the axial geogrid stiffness by 26% causes an increase in maximum axial tensile force in the reinforcement of approximately 10%. Finally, the relative deflection decreased with an increase in the L/H ratio.

Keywords: MSE wall, Constitutive models, Finite element analysis, Geogrid stiffness, Secondary reinforcement.

INTRODUCTION

In the last decades, mechanically stabilized earth (MSE) walls have become a perfect alternative for concrete retaining walls due to their capability to retain soil at a lower cost than traditional retaining walls (Bathurst et al., 2019; Ren, 2019). Furthermore, reinforcing the soil increases its stiffness. Generally, reinforced soil structures are more flexible and ductile; therefore, it is more capable of resisting seismic load and differential settlement (Bathurst et al., 1997; Holtz et al., 1997). MSE walls must be carefully designed and constructed to obtain satisfactory stability. Mechanically stabilized earth (MSE) walls consist of three components: backfill (mostly granular soil), facing unit and reinforcing element (geogrid, geotextiles, or metal strip) (Bowles, 1988; Craig, 1997; Stark et al., 2019; Rahmeyer, 2016).

MSE walls resist the lateral earth pressure through the friction between soil and reinforcement. The soil-reinforcement interaction requires a certain length of reinforcement (Berg et al., 2009; Elias, 2001).

When loads are applied to the MSE wall, the soil is compressed vertically and extends in a horizontal direction. Due to the high stiffness of the reinforcement, the deformation of the backfill soil is restrictive.

Moreover, the friction between soil and reinforcement moves the reinforcing element in a way that is compatible with the movement of the soil.

According to the American Association of State Highway and Officials (AASHTO, 2002), the recommended length is 0.7 H and the minimum length of the reinforcement element is 2.4 m (H is the height of the MSE wall). Bilgin and Kim (2010) found that using insufficient length of reinforcement results in excessive horizontal displacement for the facing of the wall and leads to failure in some cases. Soong and Koener (1999) studied the influence of the backfill soil and found that the backfill greatly affects the stability of the MSE wall. Twenty case histories were reported for the MSE wall failure due to inadequate backfill material. Backfill should not contain organic materials or harmful substances. Furthermore, the backfill should be drainage soil (Elias et al., 2001).

Many researchers studied the MSE walls and the influence of backfill on the interaction between soil and reinforcement using numerical analysis and experimental studies (Abd El Raouf, 2019; Abdelouhab et al., 2010; Bergado et al., 2003; Farrag et al., 1993; Djabri & Benmebarek, 2020; Langcuyan et al., 2017; Mosallanezhad et al., 2016; Palmeira, 2009; Lee, 2000).

Golam Kibria et al. (2014) studied the effect of reinforcement stiffness, reinforcement length, and friction angle of the backfill soil on the stability of the MSE wall using PLAXIS program. Adis Skejic et al. (2013) studied the behavior of MSE walls experimentally. The results were in good agreement with the finite element modeling results. The triangular shape of earth pressure distribution assumed by Rankine is the most common method utilized among designers.

Anand et al. (2023) studied the effect of surcharge loads and the type of reinforcement on the performance of the MSE wall. Also, they investigated the effect of piles and aggregate piers on the settlement of the wall constructed on soft clay.

Djabri and Benmebarek (2020) carried out a parametric analysis utilizing PLAXIS program to study the performance of back-to-back mechanically stabilized earth walls (BBMSEWs). This type of reinforced wall has two opposite sides (back-to-back). The parametric study included the effect of the distance between the opposing walls, the reinforcement stiffness, the backfill type, and the wall-facing type.

Chau et al. (2024) studied the effect of the reinforcement material on the behaviour of the MSE wall using a physical model and a numerical model. The study results indicated that the physical model results were in good agreement with numerical model results.

Sundaravel et al. (2024) investigated the deformation and stability of shored mechanically stabilized earth walls using finite element analysis. They carried out a sensitivity analysis on some influential parameters on the wall.

It can be realized that most of the studies focused on studying the behavior of reinforced soil walls numerically without taking into account the effect of the constitutive model on the results. However, in this study, the constitutive model was chosen based on comparing the results of the numerical model with the measured results obtained by Hatami and Bathurst (2005, 2006).

In this paper, the influence of some parameters on the horizontal displacement and axial force of the MSE wall was investigated using the finite element analysis. The studied parameters include the constitutive models, the geogrid stiffness, and the secondary reinforcement length. Moreover, the results obtained from the numerical analysis were verified by comparing them with field results.

NUMERICAL AND ANALYTICAL ANALYSIS OF MSE WALLS

The MSE wall can be analyzed and designed using the limit equilibrium method and the numerical analysis. The factor of safety of the MSE wall can be calculated by the limit equilibrium method. However, the stress distribution and deformation of the MSE wall cannot be determined using the traditional limit equilibrium method (Han & Leshchinsky, 2004). The traditional limit analysis methods were applied to several engineering projects. Recently, many software programs have been developed to design MSE walls. Many outputs (deflection, stress, strain, … etc.) can be obtained from numerical analysis, contrary to the traditional limit equilibrium method. To predict soil behavior by numerical modeling, an appropriate constitutive model must be used (Reddy & Navarrete, 2008; Kim et al., 2010; Pierson et al., 2011).

Validation of the Finite Element Model

To validate the finite element model, the results obtained in this research were compared with measured results from a full-scale experimental MSE wall investigation by Hatami and Bathurst (2005, 2006).

The Experimental MSE Wall Description

Figure (1) shows the experimental MSE wall description developed by Hatami and Bathurst (2005, 2006).

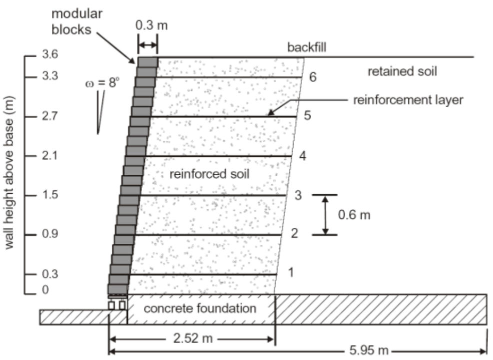

Figure (1): Configuration of the experimental MSE wall (Hatami & Bathurst, 2005, 2006)

The experimental MSE wall can be defined as follows:

The wall height is 3.6 m and the facing of the MSE wall is inclined by 8 degrees. The foundation soil is uniform beach sand with the following characteristics: unit weight (γ) =16.8 kN/m^3, friction angle (φ) = 44^o, and cohesion (C) = 1kPa. The reinforcement element is a biaxial geogrid, the axial stiffness (EA) of the geogrid layer is 115 kN/m, the ultimate strength of the geogrid is 14 kN/m, the length of the reinforcement is 2.52 m.

The facing consists of concrete modular blocks with a unit weight of 22 kN/m^3. The dimensions of the facing unit are 150mm in height, 200 mm in depth, and 300 mm in width.

DESCRIPTION OF THE NUMERICAL MODEL

PLAXIS 2D computer program was used for carrying out the analysis. A validation was performed to verify the accuracy of the finite element model. Figure (2) shows the schematic diagram of the model used in the analysis. The dimensions of the numerical model are the same as those of the experimental model, where the height equals 3.6 m. The backfill layers are simulated by 15 node elements using the hardening soil model with small strain (HSS) which is an advanced soil model used specially to simulate complex geotechnical problems. The size of the mesh in this analysis is medium with automatic mesh refinement which takes into account the necessary mesh refinement around structural elements and can reduce modeling time as well as errors during the modeling process (Bringreve et al., 2020). For the simulation of wall-facing units, 6 node plate elements were used. Foundation soil, which is rigid concrete, is simulated *via* a linear elastic model. Finally, the geogrids were simulated using geogrid elements. For modeling the soil–structure interaction, an automatic interface element is used, which is generated between wall-facing, geogrids and soil layers. The roughness of the interface (R_{int}) = 0.75 (Brinkgreve, 1998). Default time increment was used in the calculation.

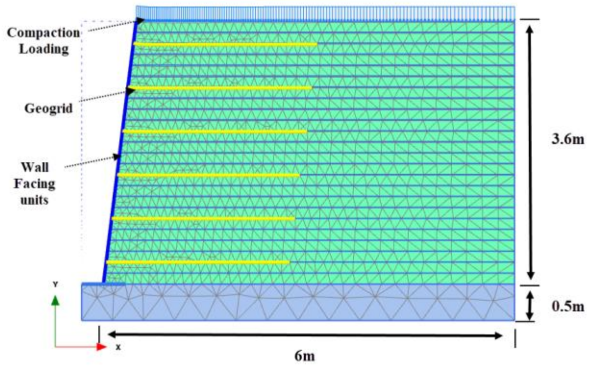

Figure (2): Schematic diagram of the numerical model

Wall construction is modeled using staged construction up to EOC (End of Construction). The stages of wall construction are divided into three steps, as follows:

- Construction of soil backfill layers of 15 cm thickness for every layer.
- Simulation of compaction loading using surcharge loading of 8 kPa magnitude at the top of each layer.
- Installation of reinforcement which consists of six geogrid layers with vertical spacing equal to 60 cm.

Properties of the Used Materials

In this analysis, the hardening soil with a small strain (HSS) model is selected to simulate the soil layers. The following parameters are required: angle of internal friction (ϕ), cohesion (C), angle of dilatancy (ψ), primary oedometer load stiffness (E_{oed}^{ref}), principal load stiffness (E_{50}^{ref}), unloading-reloading stiffness (E_{ur}^{ref}), failure ratio (R_f), unloading-reloading Poisson's ratio, power m in stiffness laws, the reference shear modulus at very small strains (G_o^{ref}). Finally, the shear strain ($\gamma_{0.7}$) at which $G_s = 0.722G_o$. Table 1 shows the values of these parameters.

The principal load stiffness E_{50}^{ref} is calculated using Equation (1).

$$E_{50}^{ref} = \left(\frac{c\cos\phi - \sigma'3\ sin\phi}{c\cos\phi - pref\ \sin\phi}\right)^m \quad (1)$$

where: c = cohesion of th soil, ϕ = angle of shearing resistance, σ′3 = minor principal effective stress, p_{ref} = reference effective confining stress and m = degree of stress dependency.

Usually, E_{ur}^{ref}~ 3, E_{50}^{ref} and E_{oed}^{ref}~ E_{50}^{ref} as recommended by Bringreve et al. (2020).

The small shear strain modulus (G_o) can be calculated using Equation (2).

$$Go = G_o^{ref}\left(\frac{c\ cos\ \phi - \sigma_3'\ \sin\phi}{c\cos\phi + pref\ \sin\phi}\right)^m \quad (2)$$

The reference shear modulus at very small strains (G_o^{ref}) can be calculated using Equation (3).

$$G_o^{ref} = 33 \text{ x } \frac{(2.97-e)2}{1+e} \text{ (MPa).} \quad (3)$$

Finally, the shear strain ($\gamma_{0.7}$) at which $G_s = 0.722G_o$ is estimated using Equation (4).

$$\gamma_{0.7} \approx \frac{1}{9\,Go}\{2c'[1+\cos(2\phi)] - \sigma_1'(1+k_o)\sin(2\phi')\} \quad (4)$$

where: k_o= coefficient of earth pressure at rest, and e= initial soil void ratio.

Table 1. The parameters used in the finite element analysis

Parameter	Value
Soil backfilling - Unit weight γ (kN/m^3)	16.8
Unit weight of MSE wall facing γ (kN/m^3)	22
E_{50}^{ref} (MPa)	48
E_{oed}^{ref} (MPa)	48
E_{eur}^{ref} (MPa)	144
υ_{ur}	0.2
Angle of backfill soil shearing resistance ϕ (°)	44
Backfill soil cohesion C (kPa)	1
Backfill soil dilation angle ψ (°)	11
Power (M) (unitless)	0.5
P_{ref} (kPa)	100
Failure ratio R_f	0.86
R_{int} (unitless)	0.75
$\gamma_{0.7}$	1.5x10^{-4}
G_o^{ref}(MPa)	150
Geogrid (EA) (kN/m)	115
Wall facing unit modulus of elasticity E (kPa)	2.0 E+06
Foundation soil (linear elastic model) E (kPa)	3.0 E+07

Comparison of Numerical Results with Measured Data

Figures (3.a) to (3.f) show the maximum axial strain (EOC) that occurred at the point where the geogrid meets the facing unit. Moreover, the axial strain decreased as we moved away from the facing unit. The end of construction (EOC) means the period from the moment at which the facing unit is placed until the end of construction. The results indicated that the strain values in the upper geogrid layers obtained from the finite element analysis and measured results are remarkably close. Furthermore, the difference between the finite element results and the measured results in the lower geogrid layers is due to the effect of the concrete foundation. Accordingly, the comparison between the finite element results and the measured results from a full-scale experimental MSE wall developed by Hatami and Bathurst (2005, 2006) indicated that the finite element results are fairly in agreement with the measured results.

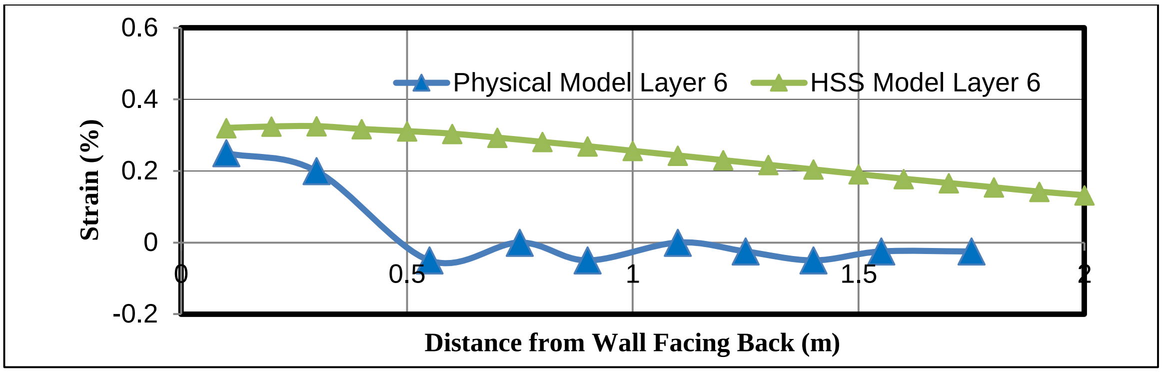

Figure (3a): The measured results at EOC *versus* numerical results for layer (6)

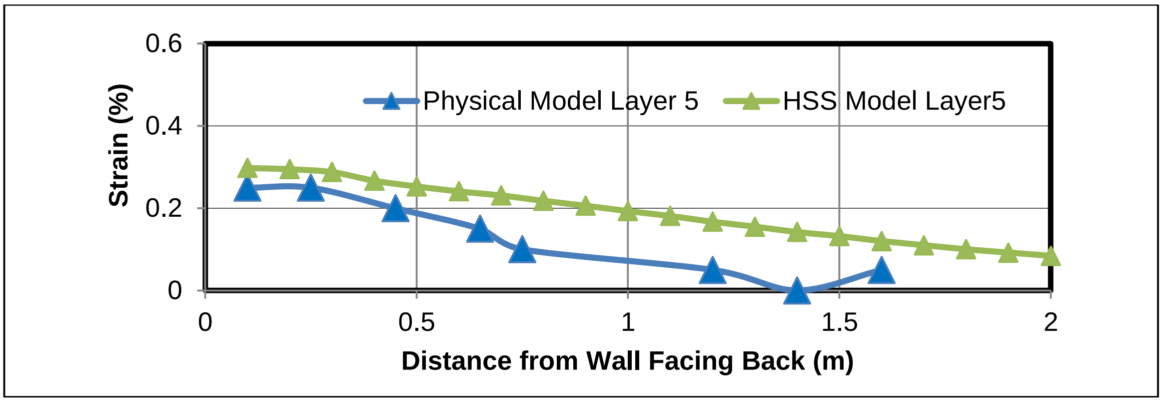

Figure (3b): The measured results at EOC *versus* numerical results for layer (5)

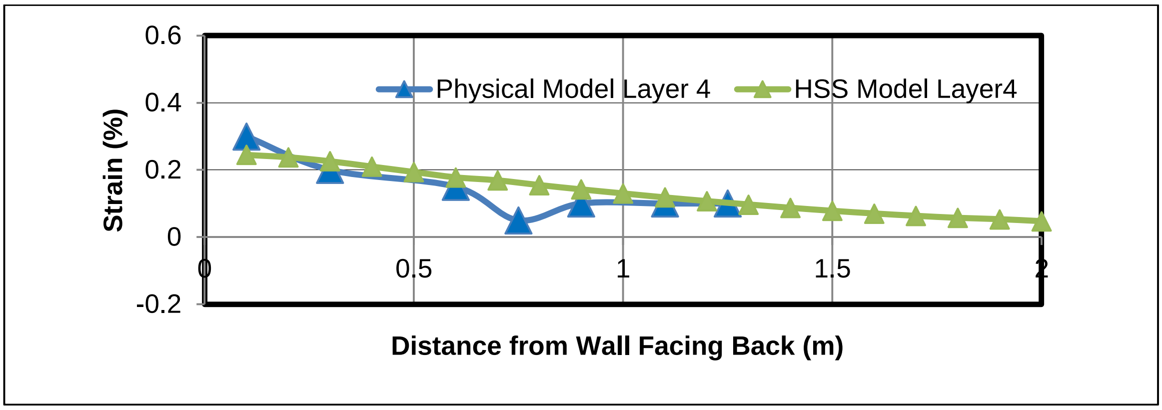

Figure (3c): The measured results at EOC *versus* numerical results for layer (4)

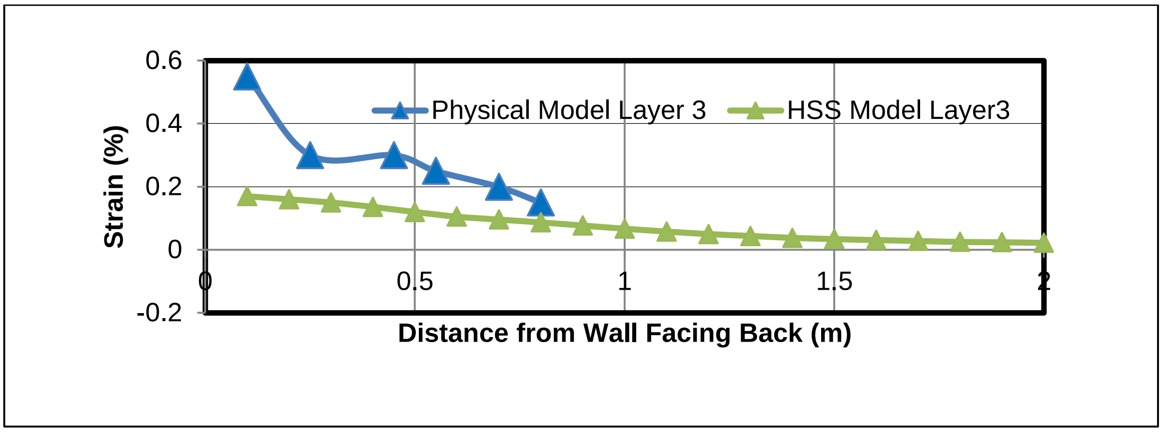

Figure (3d): The measured results at EOC *versus* numerical results for layer (3)

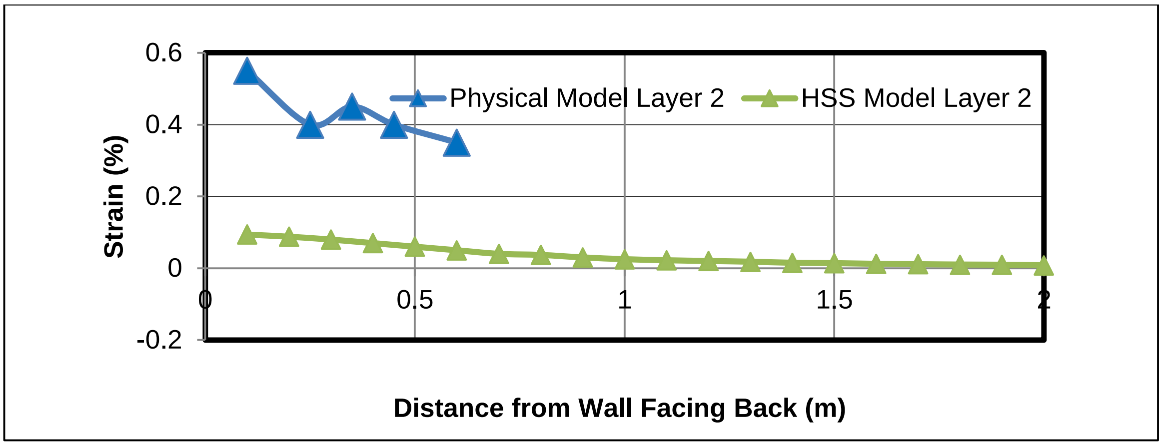

Figure (3e): The measured results at EOC *versus* numerical results for layer (2)

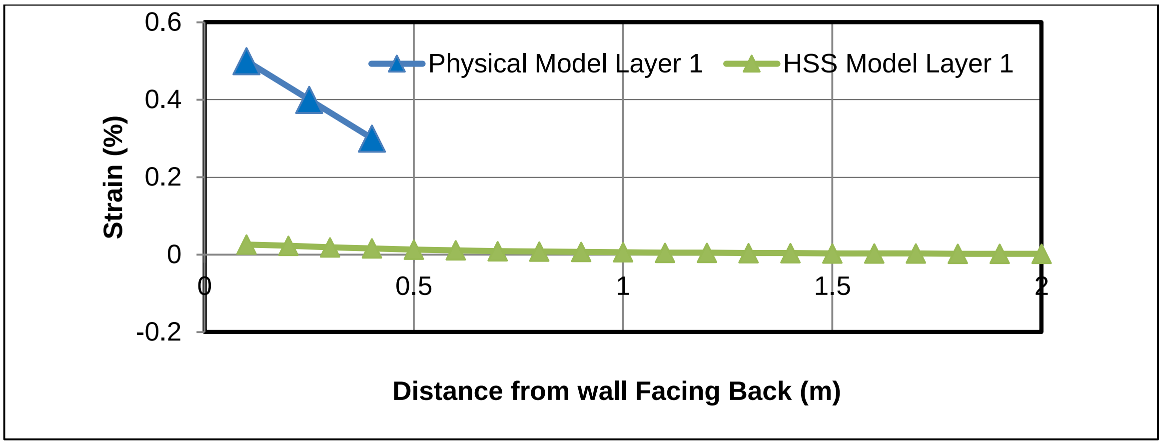

Figure (3f): The measured results at EOC *versus* numerical results for layer (1)

PARAMETRIC STUDY

In this section, the effect of the intended parameters is examined. The influence parameters were studied using the single-variable controlling method.

Effect of Constitutive Models

In order to study the influence of the constitutive models on the performance of the MSE wall, different types of constitutive models were studied, which are the hardening soil model (HS), the hardening soil with a small strain model (HSS), and Mohr-Columb model (MC).

The Mohr-Coulomb model (MC) is the perfect linear elastic-plastic model. The Mohr-Columb model involves two main parameters: the soil cohesion (c) and the friction angle (ϕ). In addition, three parameters are required: Young's modulus (E), Poisson's ratio (ν) and the dilatancy angle (ψ). The hardening soil model (HS) is the second model in use and exhibits non-linear material behavior before failure, as shown in Figure (4) (Ehsan, 2013). The soil cohesiveness (c) and the friction angle (ϕ) must be entered as part of the Mohr-Coulomb failure criterion. However, employing three separate inputs: triaxial unloading stiffness (E_{ur}), stiffnesses—triaxial loading stiffness (E_{50}), and the oedometer loading stiffness (E_{oed}) enables far more precise simulation of soil behavior. The stress-dependency of stiffness moduli, which states that all stiffnesses increase with an increase in pressure, is also taken into account by the hardening soil model.

The hardening soil model with small strain (HSS) is the third model used in this analysis. The typical HS model assumes that material behavior during unloading and reloading will be perfectly linear. However, the range of strain in which soil is considered linear is very small. With increasing strain amplitude, soil stiffness decreases non-linearly as shown in Figure (5) (Benz et al., 2009; Vermeer, 1978).

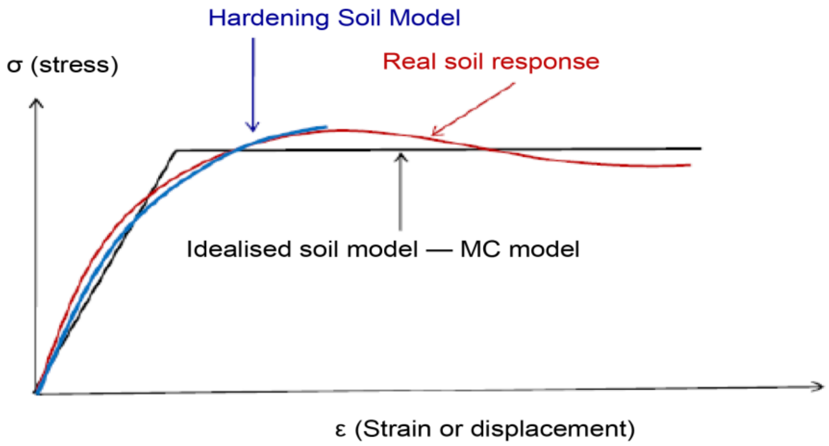

Figure (4): Comparison between HS and MC models with real soil behavior (Ehsan, 2013)

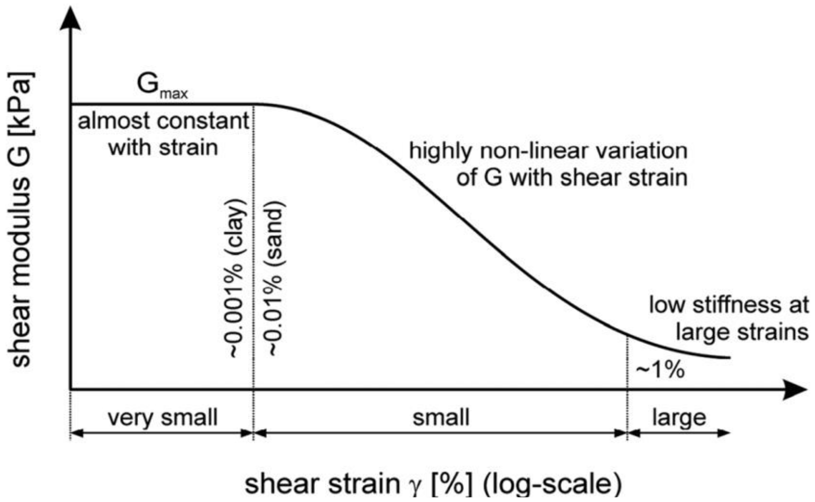

Figure (5): HSS model stiffness and shear modulus *versus* shear strain (Benz et al., 2009; Vermeer, 1978)

From Figure (6), it can be noticed that the maximum relative facing displacement when using the HSS model was 6.04 mm at a depth equal to 0.67 H. Also, the maximum relative facing displacement when using the HS model was 6.33 mm at a depth equal to 0.67H. Furthermore, the maximum relative displacement when using the MC model was 2.51 mm at a depth equal to 0.75H. The relative displacement measured by Hatami and Bathurst was 5.8mm at a depth equal to 0.75 H.

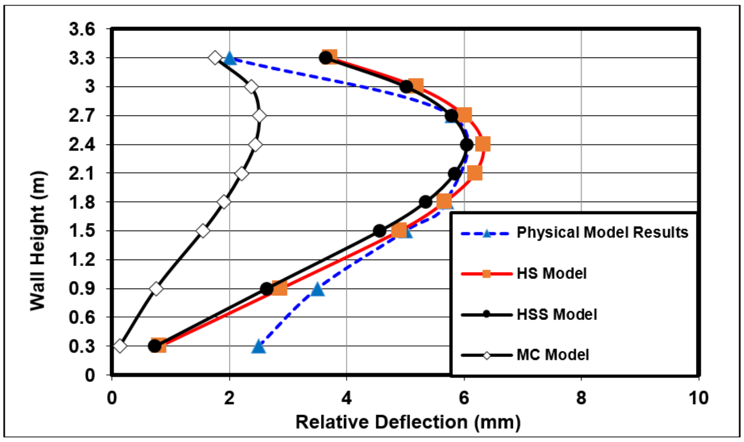

Figure (6): Constitutive models *versus* relative deflection

From Figure (7a) it can be noticed that for layer 6, the maximum strain when using HSS, HS and MC models was 0.32%, 0.19% and 0.15%, respectively, while the maximum measured strain was 0.25 %. From Figure (7b), it can be noticed that for layer 5, the maximum strain when using HSS, HS and MC models was 0.298%, 0.2 %and 0.127%, respectively, while the maximum measured strain was 0.25%. From Figure (7c), it can be noticed that for layer 4, the maximum strain when using HSS, HS and MC models was 0.245%, 0.17% and 0.095%, respectively, while the maximum measured strain was 0.3%. From Figure (7d), it can be noticed that for layer 3, the maximum strain when using HSS, HS and MC models was 0.17%, 0.11% and 0.059%, respectively, while the maximum measured strain was 0.55 %. From Figure (7e), it can be noticed that for layer 2, the maximum strain when using HSS, HS and MC models was 0.094%, 0.16% and 0.029%, respectively, while the maximum measured strain was 0.55 %. From Figure (7f), it can be noticed that for layer 1, the maximum strain when using HSS, HS and MC models was 0.026%, 0.021% and 0.08%, respectively, while the maximum measured strain was 0.50%. The numerical analysis results indicated that HSS predictions are more realistic than the results obtained from the traditional MC model and the original HS model, because the HSS model considers more material parameters than the MC model and the HS model. Furthermore, the HSS model is a modification of the original HS model, but takes into consideration the increased stiffness of soils at small strains. Therefore, at low strain levels, most soils exhibit a higher stiffness. To simulate this behavior, two additional material parameters are required: G_o^{ref} (the reference small-strain shear modulus) and $\gamma_{0.7}$ (the shear strain level at which the shear modulus has reduced to about 70% of the small- strain shear modulus, or G_s= 0.722G_o).

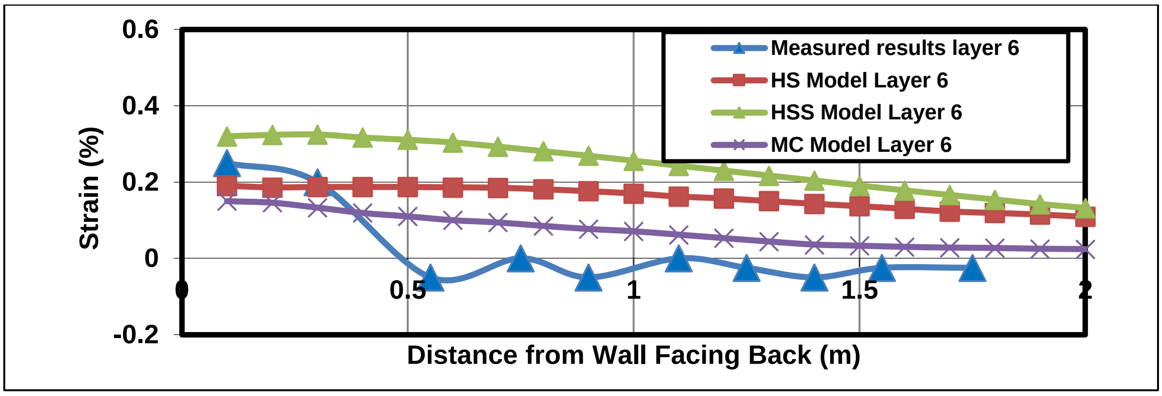

Figure (7a): The constitutive models *versus* % strain (layer 6)

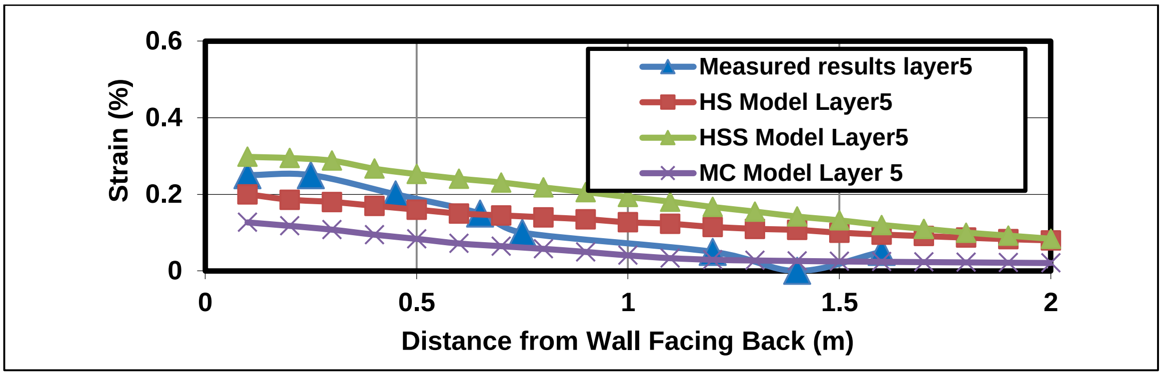

Figure (7b): The constitutive models *versus* % strain (layer 5)

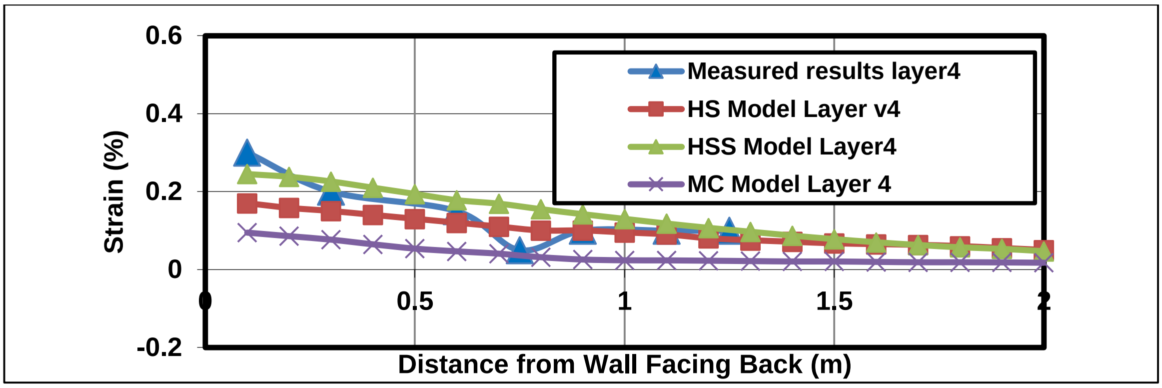

Figure (7c): The constitutive models *versus* % strain (layer 4)

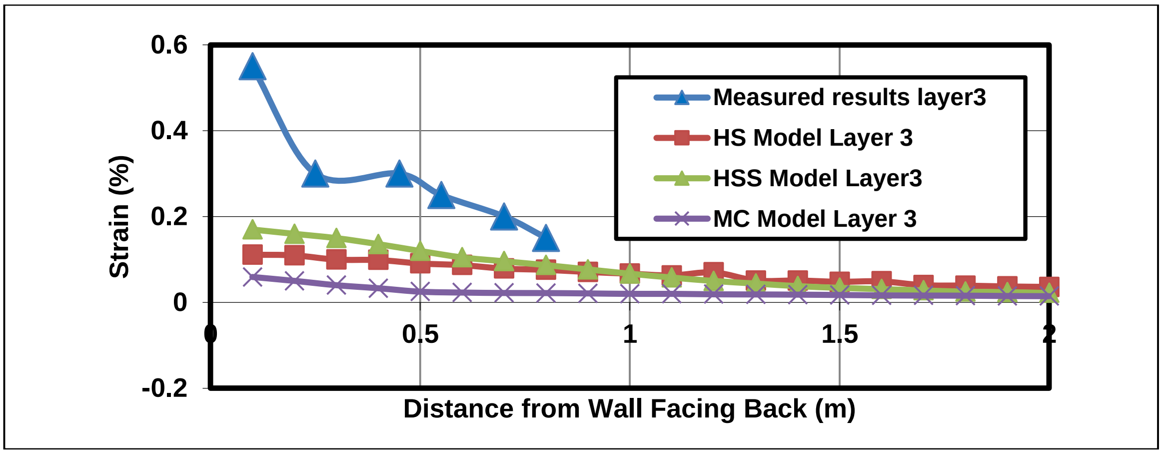

Figure (7d): The constitutive models *versus* % strain (layer 3)

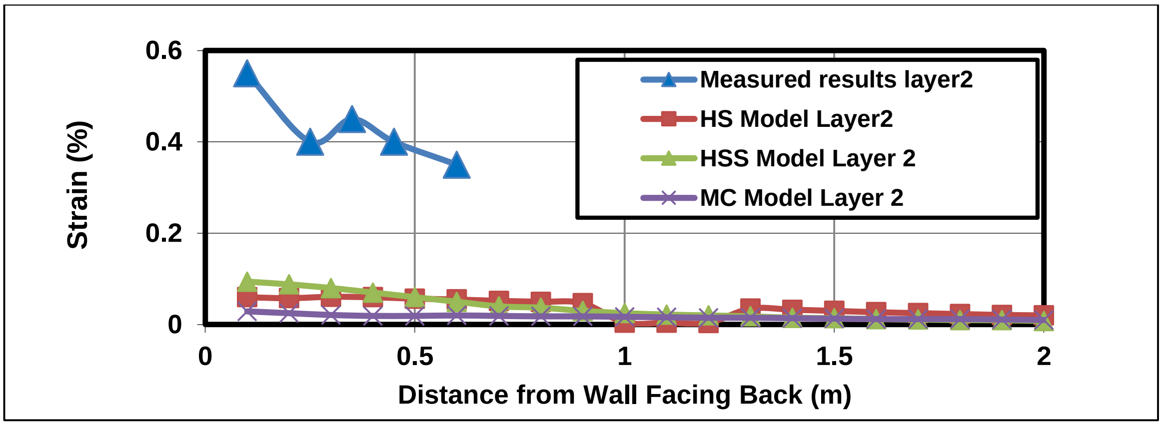

Figure (7e): The constitutive models *versus* % strain (layer 2)

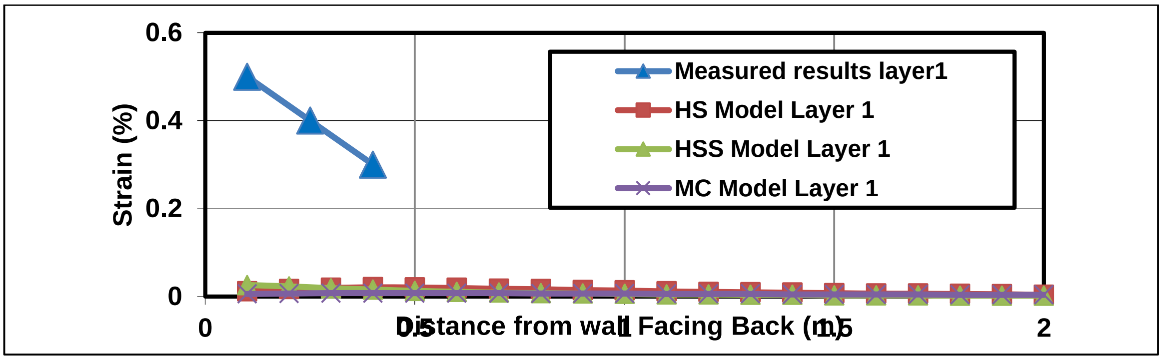

Figure (7f): The constitutive models *versus* % strain (layer 1)

Effect of the Axial Stiffness of the Geogrid (EA)

To study the influence of the axial stiffness of the geogrid (EA) on the performance of the MSE wall, several numerical analysis tests were executed. In this sub-section, all parameters were kept constant, and the stiffness of the geogrid was varied. The axial stiffness (EA) was 115 kN/m in the base model. Three additional cases were studied with axial stiffness of 125kN/m, 135kN/m and 145 kN/m, respectively.

Figure (8) indicates the profile of the relative deflection of the facing unit with different values of geogrid stiffness (EA). From the numerical analysis, it can be noticed that the geogrid stiffness (EA) had a significant effect on the relative deflection of the facing unit. Furthermore, the relative deflection of the wall facing increased with elevation, reaching its maximum roughly in the middle of the wall. After that, the relative deflection decreased with height.

Moreover, it can be noticed that the relative deflection of the facing unit decreased with an increase in the geogrid stiffness (EA). These results show the benefit of the geogrid stiffness in reducing the deflection of the facing unit.

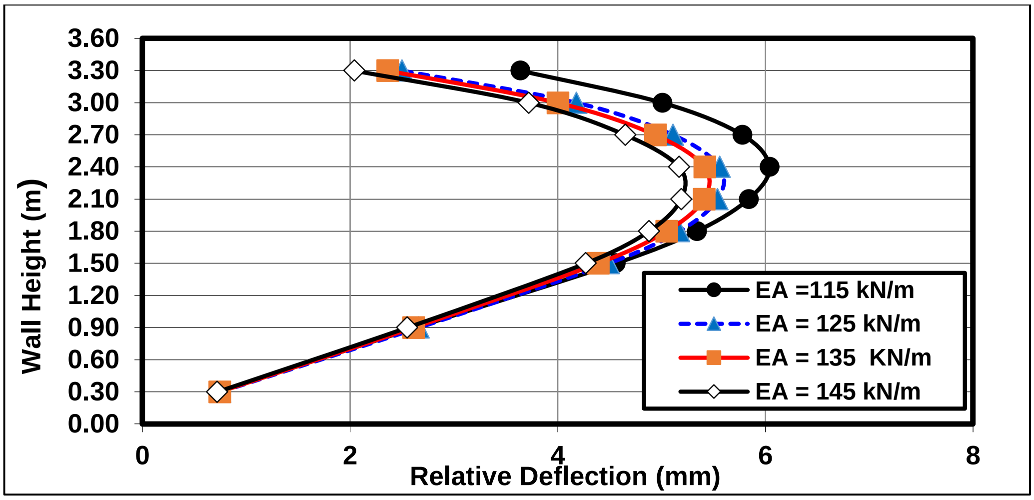

Figure (8): Effect of geogrid stiffness on relative deflection of the wall facing

Also, it can be noticed that the maximum axial force in the reinforcement for all geogrid layers occurred at a distance from the facing unit equal to 0.15 of the length of the geogrid layer. After that, the axial force decreased as we moved away from the facing unit.

To show the effect of geogrid stiffness on the axial force in the reinforcement, the relationship between maximum axial tensile force and geogrid stiffness is graphed in Figure (9). The maximum axial force increased as the geogrid stiffness increased. Moreover, increasing the geogrid stiffness by 26% caused an increase in the maximum axial force in the reinforcement by approximately 10%.

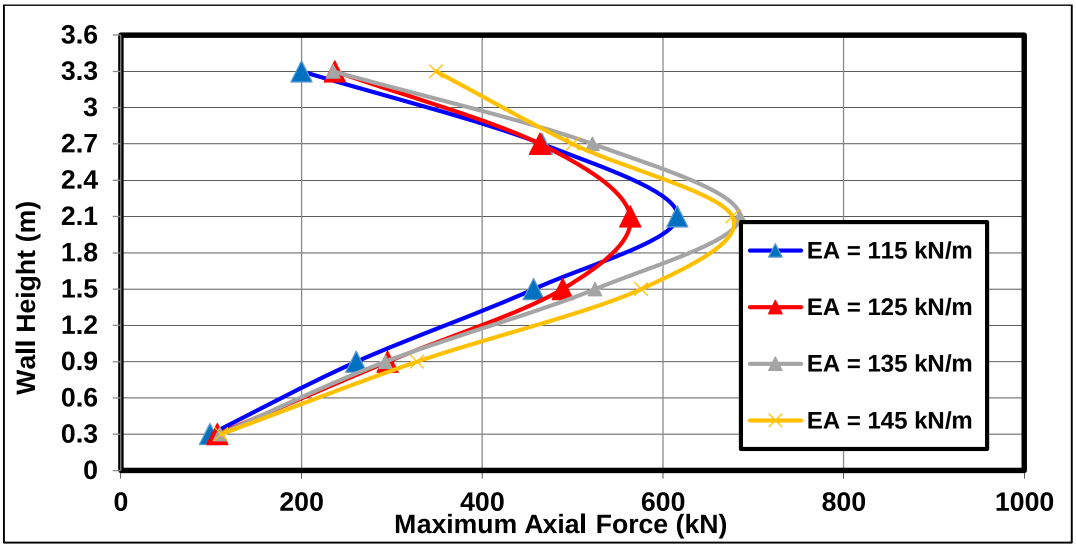

Figure (9): The geogrid stiffness *versus* maximum axial force

Effect of Secondary Reinforcement

In this sub-section, a numerical analysis was carried out to evaluate the effect of the secondary reinforcement length on the performance of the MSE wall. The secondary reinforcement was installed between the primary geogrid layers at a vertical spacing of 0.3m, as indicated in Figure (10).

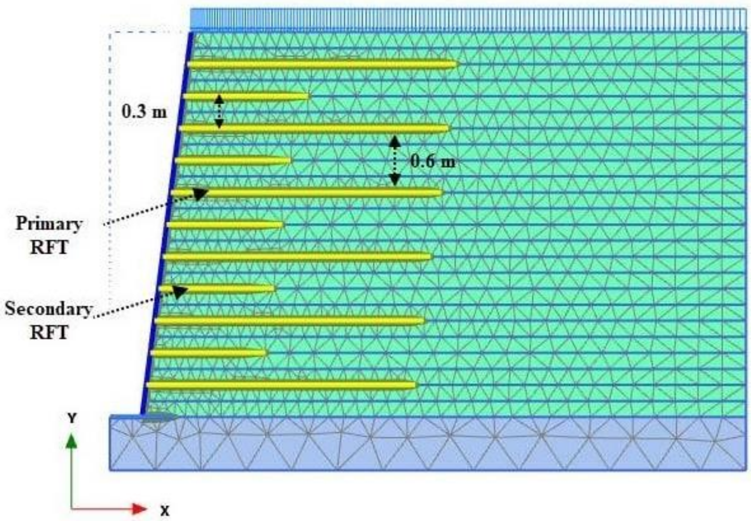

Figure (10): Position of secondary reinforcement

Figure (11) shows the displacement of the wall facing along the wall height at different L/H ratios. L= the secondary reinforcement length, and H= the wall height. The L/H ratio ranged from 0.1 to 0.5. It can be noticed that the relative deflection decreased with an increase in the L/H ratio. Moreover, the relative deflection of the wall facing increased with elevation and reached its maximum roughly in the middle of the MSE wall. After that, the relative deflection decreased with elevation. Also, the relative deflection at the bottom of the wall is almost the same value in all cases. Moreover, increasing the (L/H) ratio from 0.1 to 0.5 caused a decrease in relative deflection by approximately 11%.

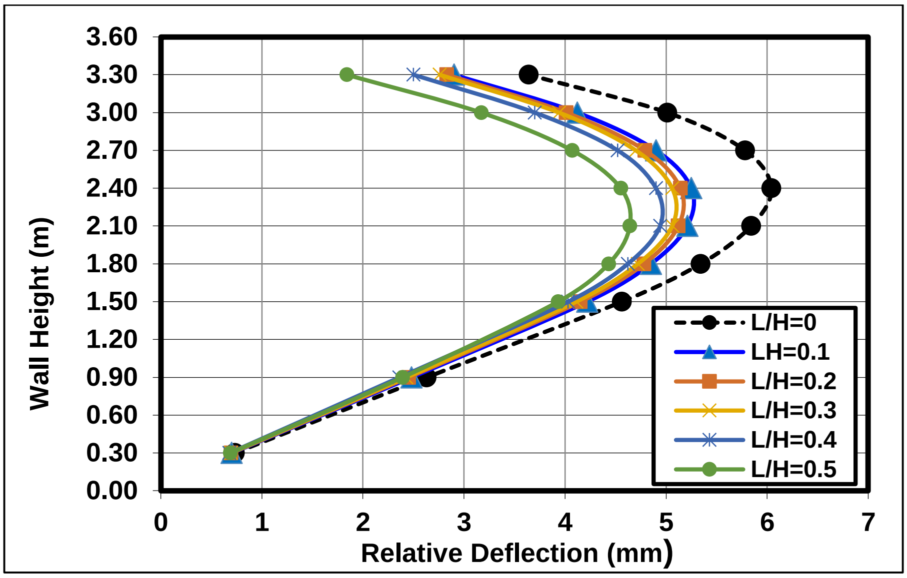

Figure (11): Effect of secondary reinforcement on relative deflection of the facing unit

To show the effect of the secondary reinforcement on the maximum axial force in the reinforcement, the relationship between the L/H ratio and the maximum force is graphed in Figure (12).

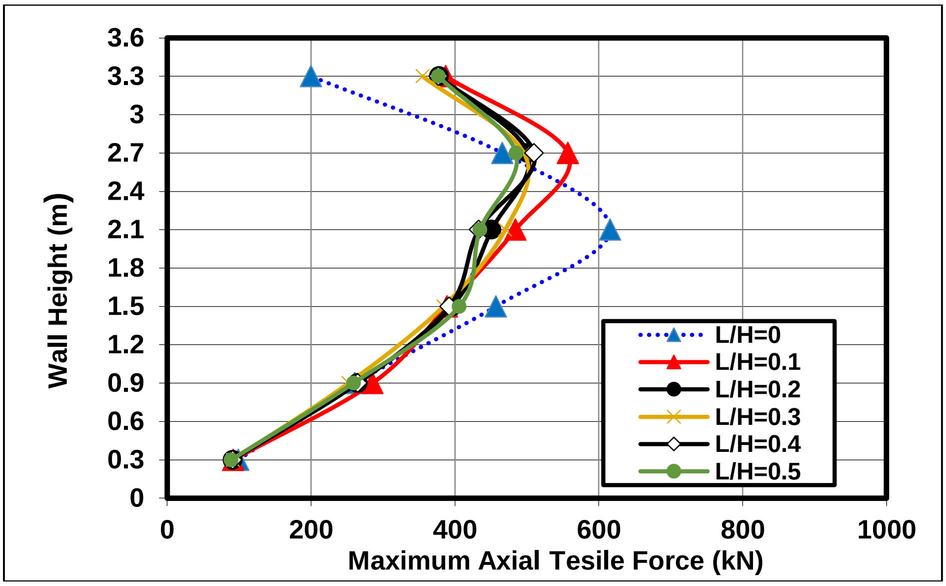

Figure (12): Effect of secondary reinforcement on maximum tensile force

The baseline model with a ratio of L/H =0 (without secondary reinforcement) was considered for comparison purposes. Generally, the secondary reinforcement caused a decrease in the maximum axial force. Moreover, for H/L=0 (case of no secondary reinforcement), the maximum axial force occurred at H/d = 0.58, where d= the height of the reinforcement layer from the bottom of the wall. When adding a secondary reinforcement, the maximum axial force occurred at H/d = 0.75. Furthermore, the maximum tensile force decreased as L/H increased. However, the L/H ratio had a limited effect on the maximum axial force.

CONCLUSIONS

The influence of some parameters on the horizontal displacement and axial force of MSE walls was investigated using the finite element analysis.

From the numerical analysis using PLAXIS 2D, the following conclusions can be drawn:

- The hardening soil model with small strain (HSS) predictions are more realistic than those of the traditional Mohr-Columb (MC) model and the hardening soil model (HS).
- The geogrid stiffness (EA) had a significant effect on the relative deflection of the facing unit. Furthermore, the relative deflection of the wall facing increased with elevation, reaching its maximum roughly in the middle of the wall. After that, the relative deflection decreased with height. Therefore, choosing the axial stiffness of the geogrid (EA) is important when designing MSE walls.
- A reduction of the relative deflection of the wall facing was observed with the increase in axial geogrid stiffness. These results show the benefit of the geogrid stiffness in reducing the deflection of the facing unit.
- The maximum axial force in the reinforcement occurred at a distance from the wall facing equal to 0.15 of the length of the geogrid layer. Also, the maximum axial force in the reinforcement increased as the geogrid stiffness increased. Moreover, increasing the geogrid stiffness by 26% caused an increase in the maximum axial force in the reinforcement by approximately 10%.
- The relative deflection decreased with an increase in the L/H ratio. Moreover, increasing the (L/H) ratio from 0.1 to 0.5 caused a decrease in the relative deflection by approximately 11%.
- The secondary reinforcement caused a decrease in the maximum axial force. Furthermore, the maximum axial force decreased as the L/H ratio increased.

REFERENCES

Abdelouhab, A., Dias, D., and Freitag, N. (2010). “Physical and analytical modeling of geosynthetic strip pull-out behavior”. Geotext. Geomembr., 28 (1), 44-53.

Abd El Raouf, M. (2019). “Compaction-induced stress in geosynthetic reinforced soil walls”. JES. Journal of Engineering Sciences, 47 (4), 451-460. doi:10.21608/jesaun.2019.109854

Adis Skejic, Anis Balic, Haris, J., Namas, S., Selman, and Emir Karamehmedovic. (2013). “Observation and numerical modeling of test MSEW with inextensible inclusions and course crushed stone backfill”. Electronic Journal of Geotechnical Engineers, 18, Bund.

Anand, M., Hulagabali, C.H., Solanki, G.R., Dodagoudar, and Anitha. (2023). “Finite-element analysis of segmental precast concrete panel reinforced earth retaining wall”. Jordan Journal of Civil Engineering, 17 (4). doi:https://doi.org/10.14525/JJCE.v17i4.03

Bathurst, R.J. (2019). “Developments in MSE wall research and design”. In: Proceedings of the International Congress and Exhibition Sustainable Civil Infrastructures. Cairo, Egypt, 10-15 November 2019; Springer: Berlin/Heidelberg, Germany, 22-50.

Bathurst, R.J., Cai, Z., Alfaro, M., and Pelletier, M. (1997). “Seismic design issues for geosynthetic-reinforced segmental retaining walls”. Proc. of the International Symposium on Mechanically Stabilized Backfill, J.T.H. Wu, ed., Balkema, Rotterdam, The Netherlands, 79-97.

Benz, T., Schwab, R., and Vermeer, P. (2009). “Small-strain stiffness in geotechnical analyses”. Bautechnik (Special Issue), 1, 6-26.

Berg, R.R., Samtani, N.C., and Christopher, B.R. (2009). “Design of mechanically stabilized earth walls and reinforced soil slopes”. Volume II, U.S. Department of Transportation. Federal Highway Administration: Washington, DC, USA.

Bergado, D., Youwai, S., Teerawattanasuk, C., and Visudmedanukul, P. (2003). “The interaction mechanism and behavior of hexagonal wire mesh-reinforced embankment with silty sand backfill on soft clay”. Comp. Geotech., 30 (6), 517-534.

Bilgin, Ö., and Kim, H. (2010). “Effect of soil properties and reinforcement length on mechanically stabilized earth wall deformations”. Proc. Earth Retention Conference 3, 556-563, ASCE. Reston, VA.

Bowles, J.E. (1988). “Foundation analysis & design”. 5th Edition, McGraw Hill, Sydney.

Brinkgreve, R.B.J. (1998). “PLAXIS 2D version 8 reference manual”. Delft University of Technology and PLAXIS bv, The Netherlands.

Brinkgreve, R.B.J. (2020). “PLAXIS 2D manual”. Delft.

Chau, Truong L., Thu-Ha Nguyen, and Van-Ngoc Pham. (2024). “Physical and numerical models of mechanically stabilized earth walls using self-fabricated steel reinforcement grids applied to cohesive soil in Vietnam”. Applied Sciences, 14 (3), 1283. https://doi.org/10.3390/app14031283

Craig, R.F. (1997). “Soil mechanics”. Spon Press, 6th Edn.

Djabri, M., and Benmebarek, S. (2020). “Numerical investigations on the behavior of back-to-back mechanically stabilized earth walls: Effect of structural components”. Jordon Journal of Civil Engineering, 14 (3).

Ehsan, R. (2013). “A study of geotechnical constitutive models used in PLAXIS 2D”. ICE G&S Papers Competition. http://www.ice.org.uk/ICE_Web_Portal/media/southeast/Competitions/Raisa-Ehsan-past-paper.pdf.

Elias, V. (2001). “Mechanically stabilized earth walls and reinforced soil slopes: Design and construction guidelines (updated version)”. U.S. Federal Highway Administration: Washington, DC, USA.

Elias, V., Christopher, B.R., and Berg, R.R. (2001). “Mechanically stabilized earth walls and reinforced soil slopes: Design and construction guidelines”. FHWA-NHI-00-043, Federal Highway Administration (FHWA), Washington DC.

Farrag, K., Acar, Y.B., and Juran, I. (1993). “Pull-out resistance of geogrid reinforcements”. Geotext. Geomembr., 12 (2), 133-159.

Golam Kibria, Md., Sahadat Hossain, and Mohammad Sadik Khan. (2014). “Influence of soil reinforcement on horizontal displacement of MSE wall”. International Journal of Geomechanics, ASCE, 14, 130-141.

Han, J., and Leshchinsky, D. (2004). “Limit equilibrium & continuum mechanics based numerical methods for analyzing stability of MSE walls”. Proc. Engineering Mechanics Conference, ASCE, Reston, VA.

Hatami, K., and Bathurst, R.J. (2005). “Development and verification of a numerical model for the analysis of geo-synthetic-reinforced soil segmental walls under working-stress conditions”. Journal of Geotechnical and Geo-environmental Engineering, ASCE, 132 (6).

Hatami, K., and Bathurst, R.J. (2006). “Numerical model for reinforced soil segmental walls under surcharge loading”. Journal of Geotechnical and Geo-environental Engineering, ASCE, 133 (6).

Holtz, R.D., Christopher, B.R., and Berg, R. (1997). “Geosynthetic engineering”. BiTech Publishers, Vancouver, 452 pages.

Kim, D., Bhowmik, S.K., and Willmer, J.L. (2010). “A case history of MSE wall failure: Finite-element modeling and evaluation”. Proc. GeoFlorida, Advances in Analysis, Modeling and Design, GSP 199, 2232-2242, Reston, VA.

Langcuyan, C.P., Park, T., Moon, S., and Won, M. (2017). “A numerical analysis on the arrangement of reinforcements in mechanically stabilized earth walls considering various wall heights”. World Congress on Advances in Structural Engineering and Mechanics (ASEM17). Ilsan(Seoul), Korea, p. 4.

Lee, W.F. (2000). “Internal stability analyses of geosynthetic reinforced retaining walls”. Doctoral Dissertation, Seattle: University of Washington.

Mosallanezhad, M., Taghavi, S.H.S., Hataf, N., and Alfaro, M.C. (2016). “Experimental and numerical studies of the performance of the new reinforcement system under pull-out conditions”. Geotext. Geomembr., 44 (1), 70-80.

Palmeira, E.M., and Milligan, G.W.E. (2009). “Scale and other factors affecting the results of pull-out tests of grids buried in sand”. Geotechnique, 39 (3), 511-524.

Pierson, M.C., Parsons, R.L., Han, J., Brennan, J.J., and Huang, J. (2011). “Influence of geogrid stiffness on shaft lateral capacities and deflections behind an MSE wall”. Proc. GeoFrontiers, GSP 3756-3765, Reston, VA.

Rahmeyer, M.J. (2016). “Developing more efficient mechanically stabilized earth (MSE) wall reinforcements”. Master Thesis, Utah State University, Logan, UT, USA.

Reddy, D.V., and Navarrete, F. (2008). “Experimental and analytical investigation of geogrid MSE walls”. Proc. From Research to Practice in Geotechnical Engineering, 277-291, ASCE, Reston, VA.

Ren, F.F., Hao, Q., and Wang, G. (2019). “Numerical comparison on deformation characteristics of the shored mechanically stabilized earth wall between reduced-scale and full-scale models”. Soil Mech. Found. Eng., 56, 302-308.

Soong, T., and Koerner, R.M. (1999). "Geosynthetic-reinforced and geocomposite drained retaining walls utilizing low-permeability backfill soil". GRI Report 24, Geosynthetic Research Institute, Folsom, PA.

Standard Specification for Highway Bridges. (2002). "7th edn". American association of State Highway and Transportation Officials AASHTO, Inc., Washington (DC).

Stark, T.D., Handy, R., and Lustig, M. (2019). "MSE wall global stability and lesson learned". In: Geo-Congress 2019: Embankments, Dams, and Slopes, American Society of Civil Engineers: Reston, VA, USA.

Sundaravel, V., Deviprasad, B., and Dodagoudar, G. (2024). "Numerical analysis of shored mechanically stabilized earth walls". International Journal of Geotechnical Engineering, 18 (2), 133-149. doi:10.1080/19386362.2024.2365061

Vermeer, P.A. (1978). "A double-yield hardening model for sand". Geotechnique, 28 (4), 413-433.